

Asymmetric Spatiotemporal Evolution of Prebiotic Homochirality

Marcelo Gleiser*

Department of Physics and Astronomy, Dartmouth College Hanover, NH 03755, USA

The role of asymmetry on the evolution of prebiotic homochirality is investigated in the context of autocatalytic polymerization reaction networks. A model featuring enantiometric cross-inhibition and chiral bias is used to study the diffusion equations controlling the spatiotemporal development of left and right-handed domains. Bounds on the chiral bias are obtained based on present-day constraints on the emergence of life on early Earth. The viability of biasing mechanisms such as weak neutral currents and circularly polarized UV light is discussed. The results can be applied to any hypothetical planetary platform.

I. INTRODUCTION

The emergence of biomolecular homochirality in prebiotic Earth is a crucial step in the early history of life [1, 5]. It is well-known that chiral selectivity plays a key role in the biochemistry of living systems: amino acids in proteins are left-handed while sugars are right-handed. However, laboratory syntheses produce racemic results. This is somewhat surprising, given that statistical fluctuations of reactants will invariably bias one enantiometer over the other [4]: even though every synthesis is *ab initio* asymmetric [7], the enantiometric excess is nevertheless erased as the reactions unfold. An important exception is the reaction by Soai and coworkers, where a small initial enantiometric excess is effectively amplified in the autocatalytic alkylation of pyrimidyl aldehydes with dialkylzincs [31]. As stressed by Blackmond [4], Soai's reaction succeeds because it features the needed autocatalytic behavior proposed originally by Frank [9] with enantiometric cross-inhibition catalysed by dimers.

It is unlikely that the specific chemistry of the Soai reaction occurred in early-Earth. However, it displays the relevant signatures of a realistic homochirality-inducing reaction network: autocatalysis, enantiometric cross-inhibition, and enzymatic enhancement performed by dimers or by larger chirally-pure chains. In the present work, we will investigate the spatiotemporal dynamics of a reaction network recently proposed by Sandars which shares these features [30]. To it, we will add an explicit chiral bias, in order to investigate the efficacy of intrinsic and extrinsic biasing mechanisms proposed in the literature. A first step in this direction can be found in the work by Brandenburg *et al.*, who studied an extension of Sandars's model including bias but no spatial dependence [24]. By intrinsic we mean either biasing effects related to fundamental physics, such as parity-violating weak neutral currents (WNC) [16, 35] or – given that we know little of early-Earth's prebiotic chemistry and even less of other possible life-bearing planetary platforms [25] – to some as yet unknown chemical process. By extrinsic we mean possible environmental influences, such as circularly-polarized UV light (CPL) from, for example, active star-formation regions [23] or direct seeding of chiral compounds by meteoritic bombardment [8, 26]. The spatiotemporal dynamics of the reaction network will be shown to be equivalent to a two-phase system undergoing a symmetry-breaking phase transition characterized by the formation of competing domains of opposite chirality. The evolution of the domain network is sensitive to Earth's early environmental history and to the magnitude of the chiral bias. Using the time-scale associated with the emergence of life on Earth it is possible to obtain a lower bound on the bias. In particular, it will be shown that the very small bias from WNC is inefficient to generate homochiral conditions. For CPL the situation is less clear due to uncertainty in the nature and duration of sources, but still highly unlikely. The formalism is set up to be applicable to any planetary platform.

The paper is organized as follows: In section 2 we introduce the biased polymerization model and its pertinent rate equations. In section 3 we describe the reduced ($n = 2$) model and how the net chirality can be interpreted as a continuous order parameter satisfying an effective potential. This allows us to introduce explicitly spatial dependence in the study of biased polymerization. In section 4 we describe the dynamics of homochirality using techniques from the theory of phase transitions with mean-field Ginzburg-Landau models in the limit of no bias. In section 5 we generalize our results to include a small bias, describing in detail the wall dynamics in this case and the time-scales associated with the development of homochirality in early-Earth. We also investigate if the onset of prebiotic homochirality on early-Earth could have been the result of a nucleation event. We conclude in section 6 with a summary of our results and an outlook to future work.

*Electronic address: gleiser@dartmouth.edu

II. MODELING BIASED POLYMERIZATION

Sandar's model describes how long chains of homochiral polymers may evolve from a gradual build up of chiral monomers [30]. In order to reach homochirality two processes are needed: reactions must be autocatalytic so that longer, chirally-pure chains may be synthesized. In addition, a mechanism for chiral amplification is also needed. This amplification may be achieved in a number of ways [1, 16, 27]. Sandars included both enantiometric cross-inhibition and an enzymatic enhancement catalysed by the longest chain in the reactor pool.

Consider a polymer with n left-handed monomers, L_n . It may grow by aggregating a left-handed monomer L_1 or it may instead be inhibited by the addition of a right-handed monomer R_1 to either of its ends. Writing the reaction rates as k_S and k_I , the reaction network can be written as [30]:



supplemented by the four opposite reactions for right-handed polymers by interchanging $L \leftrightarrow R$. The network includes a substrate S from where both left and right-handed monomers are generated. The rate at which monomers are generated may depend on several factors. It may be due to already existing polymers with an enzymatic enhancement denoted here by $C_{L(R)}$ for left(right)-handed monomers. Sandars wrote $C_L = L_N$ and $C_R = R_N$, where N is the largest polymer in the substrate. If $N = 2$, the case we investigate here, we can model the catalytic role of dimers [4]. Wattis and Coveney [34] proposed instead $C_L = \sum L_n$ and $C_R = \sum R_n$, while Brandenburg *et al.* [24] suggested a weighted sum, $C_L = \sum nL_n$ and $C_R = \sum nR_n$. Motivated by mathematical simplicity and by Soai's reactions, we will follow Sandars.

Another factor that may influence the production rate of monomers is an explicit bias towards a specific handedness. We assign a chiral-specific reaction rate $k_{L(R)}$ such that the generation of left and right-handed monomers from the substrate S is written as



The reaction rates are related to the equilibrium population of each handedness as $k_L \propto \exp[-E_L/k_B T]$ and $k_R \propto \exp[-(E_L + E_f)/k_B T]$, where k_B is Boltzmann's constant, T is the temperature, and E_f denotes the energy difference between the two enantiomers, here chosen arbitrarily to suppress the right-handed monomers. Note that similar results would have been obtained by considering $E_{L(R)}$ to be the activation energy for forming $L(R)$ molecules, and E_f the difference in activation energy between enantiomers.

Kondepudi and Nelson [17] used a similar parameterization to express the bias due to parity violation in the weak nuclear interactions, which has been estimated to be $g \equiv E_f/k_B T \sim 10^{-17-18}$ at room temperature [3, 22, 29]. On the other hand, CPL biasing depends on a number of unknowns such as the nature of the UV source, its distance and duration and it's harder to estimate [2, 17]. Since in general $g \ll 1$, one obtains $k_L/k_R \simeq 1 + g$. Introducing the average reaction rate $k_C \equiv \frac{k_L + k_R}{2}$, we can express the left and right-handed reaction rates as

$$\begin{aligned}
 k_L &= k_C(1 + g/2) + \mathcal{O}(g^2) \\
 k_R &= k_C(1 - g/2) + \mathcal{O}(g^2) .
 \end{aligned} \tag{3}$$

If the concentration of the substrate $[S]$ is maintained by a source Q , it will obey the equation,

$$\frac{d[S]}{dt} = Q - (Q_L + Q_R) , \tag{4}$$

where $Q_{L(R)}$ are the sources for left(right)-handed monomers. From eqs. 2 and 3, the sources can be written as

$$\begin{aligned}
 Q_L &= k_C(1 + g/2)[S](pC_L + qC_R) \\
 Q_R &= k_C(1 - g/2)[S](pC_R + qC_L) ,
 \end{aligned} \tag{5}$$

where we introduced the fidelity f of the enzymatic reactions, written in terms of p and q as $p \equiv (1 + f)/2$ and $q \equiv (1 - f)/2$. In the absence of bias ($g = 0$), the fidelity f controls the evolution of the net enantiometric excess.

As has been thoroughly discussed in the literature [18, 24, 30, 34], the dynamical system defined by the polymerization equations for a given value of N shows a bifurcation behavior at a certain critical value of f , f_c . The specific value of f_c depends on the choice made for the enzymatic enhancements $C_{L(R)}$ and on the ratio of reaction rates k_I/k_S , but the behavior is qualitatively the same. Brandenburg *et al.*, with $k_I/k_S = 1$, obtained $f_c \simeq 0.38$, with f_c increasing with weaker cross-inhibition. In the limit $k_I \rightarrow 0$, $f_c \rightarrow 1$ and no enantiometric excess develops [24].

The full set of reaction rate equations governing the behavior of an n -polymer ($n = 1, \dots, N$) system consists of the following equations [24, 30]: the equation for the substrate concentration, eq. 4; the equations for the left and right monomers,

$$\begin{aligned} \frac{d[L_1]}{dt} &= Q_L - \lambda_L[L_1], \\ \frac{d[R_1]}{dt} &= Q_R - \lambda_R[R_1], \end{aligned} \quad (6)$$

where

$$\begin{aligned} \lambda_L &= 2k_S \sum_{n=1}^{N-1} [L_n] + 2k_I \sum_{n=1}^{N-1} [R_n] \\ &+ k_S \sum_{n=2}^{N-1} [L_n R_1] + k_I \sum_{n=2}^{N-1} [R_n L_1], \end{aligned} \quad (7)$$

and

$$\begin{aligned} \lambda_R &= 2k_S \sum_{n=1}^{N-1} [R_n] + 2k_I \sum_{n=1}^{N-1} [L_n] \\ &+ k_S \sum_{n=2}^{N-1} [R_n L_1] + k_I \sum_{n=2}^{N-1} [L_n R_1]; \end{aligned} \quad (8)$$

and, finally, the rate eqns. for $n \geq 2$,

$$\frac{d[L_n]}{dt} = 2k_S[L_1] ([L_{n-1}] - [L_n]) - 2k_I[L_n][R_1], \quad (9)$$

supplemented by the ones obtained substituting $L \rightarrow R$. The factors of 2 on the rhs reflect that monomers may attach to either end of the chain. For $n = 2$, however, one must discount this for the interaction of 2 single monomers.

III. REDUCED BIASED MODEL

Previous authors [24, 30, 34] have explored the evolution of the reaction network for different values of N . Here, we are interested in investigating not only the temporal evolution of the various concentrations ($[L_n]$, $[R_n]$) but also their spatial behavior in the presence of bias. We are motivated by interesting work by Saito and Huyga [28], who investigated spatial proliferation of left and right-handed polymers in the context of equilibrium Monte-Carlo methods and, in particular, by that of Brandenburg and Multamäki [6] (henceforth BM), where the spatiotemporal evolution of left and right-handed reaction networks was investigated in the absence of chiral bias.

A. Biased Polymerization Equations

As remarked by Gayathri and Rao [10], taking the concentrations to be functions of position implies that the number of molecules per unit volume is assumed to be large enough so that the concentrations vary smoothly with space and time. In other words, the concentrations are defined in a coarse-grained volume which, of course, must be larger than the smallest relevant distance-scale (ξ), to be derived below. The chemical mixture is then defined in block-volumes which are multiples of $\sim \xi^3$. This is essentially the procedure adopted in studying mean-field models of phase transitions in the Ising universality class as, for example, in ferromagnetic phase transitions, where the order parameter is the coarse-grained magnetization over a block of spins [21]. Indeed, in a recent work [12] Gleiser and Thorarinson (GT) demonstrated that chiral symmetry breaking in the context of the continuous model of BM can be

understood in terms of a second-order phase transition with a critical “temperature” determined by the strength of the coupling between the reaction network and the external environment. One cannot speak consistently of symmetry breaking without including spatial dependence.

Adding spatial dependence to the reaction network greatly complicates its study, as we must investigate coupled PDEs as opposed to ODEs. Fortunately, as remarked by BM, it is possible to truncate the system to $N = 2$ and still capture its essential behavior, the dynamics leading (or not) to homochirality within a large volume $\mathcal{V} \gg \xi^3$. Given the catalytic role of dimers in the Soai reaction [4] we will investigate the biased spatiotemporal dynamics of reaction networks with $N = 2$.

The great practical advantage of the truncation is that it elegantly reduces the system to an effective scalar field theory, where the field – the order parameter – determines the net chirality in a given volume [6].

The reaction network is further simplified by assuming that the rate of change of $[L_2]$ and $[R_2]$ is much slower than that of $[L_1]$ and $[R_1]$. The same for the substrate $[S]$, so that $d[S]/dt = Q - (Q_L + Q_R) \simeq 0$. This approximation is known as the adiabatic elimination of rapidly adjusting variables [15]: the typical time-scale for changes in the concentrations of larger chains such as $[L_2]$ and $[R_2]$, which depend on (or are enslaved by) the concentrations of $[L_1]$ and $[R_1]$, are slower than those for the concentrations $[L_1]$ and $[R_1]$ themselves. This approximation breaks down in the unlikely situation where the syntheses of dimers and higher chains have similar time-scales as those for monomers.

Using the adiabatic approximation in eq. 9 for $n = 2$, we can express the concentrations $[L_2]$ and $[R_2]$ in terms of the concentrations for the monomers as

$$[L_2] = \frac{[L_1]^2}{2[L_1] + 2k_S/k_I[R_1]}; [R_2] = \frac{[R_1]^2}{2[R_1] + 2k_S/k_I[L_1]} . \quad (10)$$

Also, using eq. 4 with $C_L = [L_2]$ and $C_R = [R_2]$, the equations for the monomers can be written as

$$\begin{aligned} \frac{d[L_1]}{dt} &= Q \frac{(1 + g/2)(p[L_2] + q[R_2])}{([L_2] + [R_2]) \left[1 + \frac{g}{2} f \left(\frac{[L_2] - [R_2]}{[L_2] + [R_2]}\right)\right]} - \lambda_L [L_1] \\ \frac{d[R_1]}{dt} &= Q \frac{(1 - g/2)(p[R_2] + q[L_2])}{([L_2] + [R_2]) \left[1 + \frac{g}{2} f \left(\frac{[L_2] - [R_2]}{[L_2] + [R_2]}\right)\right]} - \lambda_R [R_1] . \end{aligned} \quad (11)$$

Since $g \ll 1$, we can expand the rhs of eqs. 11 and greatly simplify the equations for the monomers. Once we substitute eqns. 10 into eqns. 11 we are left with two equations for the two unknowns, $[L_1]$ and $[R_1]$.

It is useful at this point to introduce the dimensionless symmetric and asymmetric variables, $\mathcal{S} \equiv X + Y$ and $\mathcal{A} \equiv X - Y$, where $X \equiv [L_1](2k_S/Q)^{1/2}$, and $Y \equiv [R_1](2k_S/Q)^{1/2}$ are dimensionless concentrations. We can thus add and subtract the equations for the monomers in order to obtain the equations satisfied by the variables \mathcal{S} and \mathcal{A} , respectively. After some algebra we get, for $k_S/k_I = 1$, the biased polymerization equations,

$$\begin{aligned} \lambda_0^{-1} \frac{d\mathcal{S}}{dt} &= 1 - \mathcal{S}^2 \\ \lambda_0^{-1} \frac{d\mathcal{A}}{dt} &= 2f \frac{\mathcal{S}\mathcal{A}}{\mathcal{S}^2 + \mathcal{A}^2} - \mathcal{S}\mathcal{A} + \frac{g}{2} \left[1 - 4f^2 \left(\frac{\mathcal{S}\mathcal{A}}{\mathcal{S}^2 + \mathcal{A}^2} \right)^2 \right] , \end{aligned} \quad (12)$$

where the parameter $\lambda_0 \equiv (2k_S Q)^{1/2}$, has dimension of inverse time. $\mathcal{S} = 1$ is a fixed point: the system will tend towards this value at time-scales of order λ_0^{-1} , independently of g . With $\mathcal{S} = 1$ and $g = 0$, the equation for the chiral asymmetry has fixed points at $\mathcal{A} = 0, \pm \sqrt{2f - 1}$. An enantiometric excess is only possible for $f > f_c = 1/2$.

Setting $\mathcal{S} = 1$, the equation for \mathcal{A} can be written as $\lambda_0^{-1} \dot{\mathcal{A}} = -\partial V / \partial \mathcal{A}$, where the dot denotes time derivative. The “potential” V controlling the evolution of \mathcal{A} is an asymmetric double-well, (symmetric for $g = 0$)

$$V(\mathcal{A}) = \frac{\mathcal{A}^2}{2} - f \ln(1 + \mathcal{A}^2) - \frac{g}{2} \mathcal{A} - gf^2 \left[\frac{\mathcal{A}}{1 + \mathcal{A}^2} - \arctan(\mathcal{A}) \right] . \quad (13)$$

In figure 1 we show the potential $V(\mathcal{A})$ for various values of the fidelity f and the asymmetry g . Note that complete chiral separation occurs only for $f = 1$ and is forbidden for $f \geq 1/2$ (left). The presence of asymmetry ($g \neq 0$, right) clearly biases one of the chiralities, leaving the minima at $\mathcal{A} = \pm 1$ unchanged for $f = 1$.

B. Introducing Spatial Dependence

In order to introduce spatial dependence for the concentrations, we follow the usual procedure in the phenomenological treatment of phase transitions [14, 21], by rewriting the total time derivatives in eqs. 12 as $d/dt \rightarrow \partial/\partial t - k\nabla^2$,

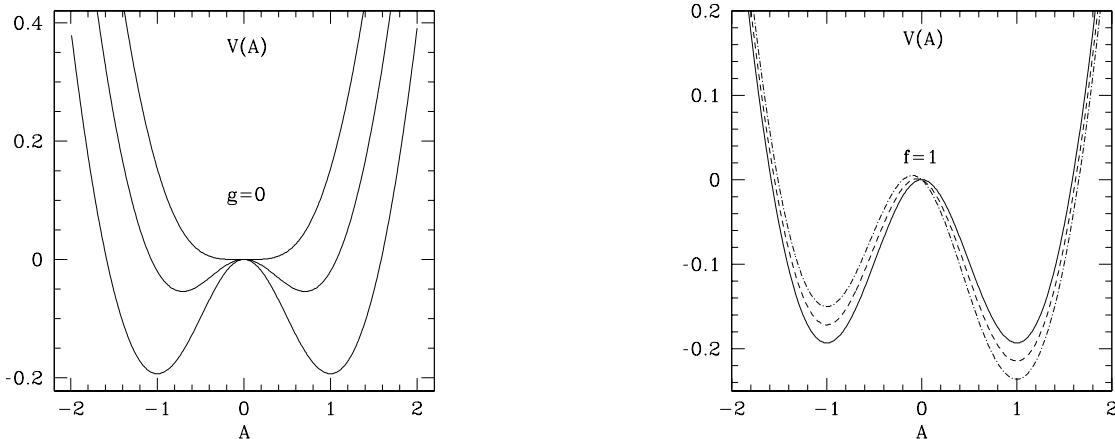


FIG. 1: Left: Potential $V(\mathcal{A})$ for $g = 0$ and varying fidelity f . From bottom to top, $f = 1, 0.75, 0.5$. Right: Potential for $f = 1$ and varying asymmetry g . The bold line corresponds to the symmetric case, $g = 0$. The dash line to $g = 0.1$ and the dot-dash line to $g = 0.2$.

where k is the diffusion constant. Some illustrative values of k are: $k = 10^{-9} \text{m}^2 \text{s}^{-1}$ for molecular diffusion in water and $k = 10^{-5} \text{m}^2 \text{s}^{-1}$ for air. The diffusion time-scale in a length L is $\tau_{\text{diff}} = L^2/k$.

It is convenient to introduce the dimensionless time and space variables, $t_0 \equiv \lambda_0 t$ and $x_0 \equiv x \sqrt{\lambda_0/k}$, respectively. The equations are then solved in terms of the dimensionless variables. Dimensionful values are obtained for particular choices of the parameters k_S , Q , and k . For example, using as nominal values $k_S \sim 10^{-25} \text{cm}^3 \text{s}^{-1}$, $Q \sim 10^{15} \text{cm}^{-3} \text{s}^{-1}$ and k for water, one obtains, $t \simeq 2.3 \times 10^{-3} t_0$ y and $x \simeq 8.5 \times 10^{-3} x_0 \text{m}$, while $\lambda_0 \simeq \sqrt{2} \times 10^{-5} \text{s}^{-1}$.

The main consequence of introducing spatial dependence is that now the net chiral asymmetry will evolve in both space and time. With a racemic or near-racemic initial distribution, a typical spatial volume $\mathcal{V} \gg \xi^3$ will coarsen into domains of left and right-handed polymers, separated by an interface or domain wall with approximate thickness $\sqrt{k/\lambda_0}$: an initially racemic solution gradually separates into chiral domains. The “wall” between homochiral domains is to be interpreted as the region of space which remains racemic [$\mathcal{A}(\mathbf{x}, t) = 0$.] In order for an initially racemic mix to evolve toward homochirality, the walls separating the left and right domains must move. We will discuss in detail below what physical processes may trigger the wall mobility.

In one spatial dimension, and for $f = 1$ and $g = 0$, the solution is well approximated by a “kink” profile obtained in the static limit ($\dot{\mathcal{A}} = 0$) as $\mathcal{A}_k(x) = \tanh(-\alpha x \sqrt{\lambda_0/k})$, where α can be found numerically to be $\alpha \simeq 0.58$ [6].

Using the dimensionless variables defined above, the energy of a static spatially-extended configuration in d spatial dimensions is given by $E[\mathcal{A}] = (k/\lambda_0)^{d/2} \int d^d x_0 [\frac{1}{2} \nabla_0 \mathcal{A} \cdot \nabla_0 \mathcal{A} + V(\mathcal{A})]$, where appropriate boundary conditions must be imposed.

IV. CHIRAL SELECTION AS A PHASE TRANSITION I: NO BIAS

Gleiser and Thorarinson coupled the net chirality $\mathcal{A}(\mathbf{x}, t)$ to an external environment modeled by a stochastic force ($\zeta(t, \mathbf{x})$) with zero mean ($\langle \zeta \rangle = 0$) and two-point correlation function $\langle \zeta(\mathbf{x}', t') \zeta(\mathbf{x}, t) \rangle = a^2 \delta(\mathbf{x}' - \mathbf{x}) \delta(t' - t)$, where a^2 measures the strength of the environmental influence. For example, in Brownian motion, $a^2 = 2\gamma k_B T$, where γ is a viscosity coefficient. With the dimensionless variables introduced above, the noise amplitude scales as $a_0^2 \rightarrow \lambda_0^{-1} (\lambda_0/k)^{d/2} a^2$. Notice that by writing $\gamma = \lambda_0 \gamma_0$ and identifying the noise amplitudes, $2(\lambda_0 \gamma_0)(k_B T) = \lambda_0 (k/\lambda_0)^{d/2} a_0^2$, we obtain that the thermal energy, $k_B T$, has dimensions of $(k/\lambda_0)^{d/2}$ and thus of $[\text{length}]^d$ as it should. The equations of motion in the presence of noise and no bias are

$$\lambda_0^{-1} \left(\frac{\partial \mathcal{S}}{\partial t} - k \nabla^2 \mathcal{S} \right) = 1 - \mathcal{S}^2 + \lambda_0^{-1} \xi(\mathbf{x}, t) \quad (14)$$

$$\lambda_0^{-1} \left(\frac{\partial \mathcal{A}}{\partial t} - k \nabla^2 \mathcal{A} \right) = 2f \frac{\mathcal{S} \mathcal{A}}{\mathcal{S}^2 + \mathcal{A}^2} - \mathcal{S} \mathcal{A} + \lambda_0^{-1} \xi(\mathbf{x}, t). \quad (15)$$

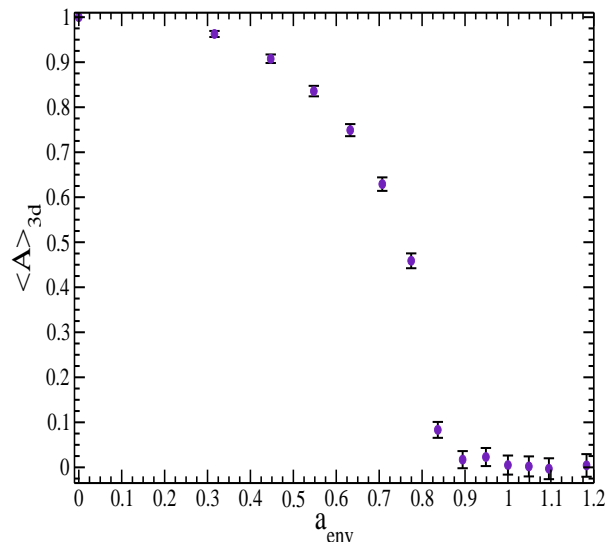


FIG. 2: Phase diagram for the 3d volume-averaged net chirality $\langle \mathcal{A} \rangle_{3d}$ as a function of external noise a_{env} . The error bars denote ensemble averaging over 20 runs.

A. Critical Point for Chiral Symmetry Breaking

As shown by GT, in the absence of chiral bias and with $f = 1$ and $\mathcal{S} = 1$ (an attractor in phase space), the system described by eq. 14 has critical behavior controlled by the noise amplitude a^2 . For a above a critical value, a_c , $\langle \mathcal{A} \rangle \rightarrow 0$ and the chiral symmetry is restored. The brackets denote spatial averaging, $\langle \mathcal{A} \rangle = (1/V) \int \mathcal{A} d^3x$, where V is the volume. In analogy with ferromagnets, where above a critical temperature the net magnetization is zero, one may say that above a_c the stochastic forcing due to the external environment overwhelms any local excess of L over R enantiomers: racemization is achieved at large scales and chiral symmetry is restored throughout space. Thus, the history of chirality on Earth and on any other planetary platform is inextricably enmeshed with its early environmental history. Although in the present work we will only consider the case of “gentle” (diffusive) evolution of the reaction network, it should be noted that “violent” disturbances may greatly affect the results and, thus, the final net chiral excess. Preliminary results for 2d turbulent stirring have been recently presented, showing that indeed it may accelerate the emergence of a final homochiral state [6]. We are presently pursuing an alternative approach wherein the interactions with the environment are modelled stochastically (cf. eqs. 14 above) and hope to report on our results shortly.

The equation dictating the evolution of the enantiometric excess \mathcal{A} was solved with a finite-difference method in a 1024^2 grid and a 100^3 grid with $\delta t = 10^{-3}$ and $\delta x = 0.2$, and periodic boundary conditions. In 2d, this corresponds to simulating a shallow pool with linear dimensions of $\ell \sim 200\text{cm}$. In order to obtain the value of a_c , the system was prepared initially in a homochiral phase chosen to be $\langle \mathcal{A} \rangle(t = 0) = 1$. The equation was then solved for different values of the external noise amplitude, a . As shown in GT, for $a^2 > a_c^2 \simeq 0.65(k/\lambda_0)^{3/2}$, $\langle \mathcal{A} \rangle \rightarrow 0$, that is, the system becomes racemized. $\langle \mathcal{A} \rangle$ approaches a constant for large times, indicating that the reaction network reaches equilibrium with the environment. For $d = 2$, $a_c^2 \simeq 1.15(k/\lambda_0)$. In figure 2 we show the phase diagram for chiral symmetry restoration in 3d.

B. Ginzburg Criterion in the Absence of Chiral Bias

It is possible to gain much insight into the relationship between the microscopic and mean-field approaches using the Ginzburg criterion [19]. With $g = 0$ and $f = 1$, the potential $V(\mathcal{A})$ is a symmetric double-well with minima at $\mathcal{A}_{\pm} = \pm 1$ and a maximum at $\mathcal{A} = 0$. $\mathcal{A} = \mathcal{A}_{\pm}$ are fixed points: if the system is prepared away from them, it will evolve towards them. When domains of both phases are present, they will be separated by domain walls. In the

absence of bias ($g = 0$) and of environmental coupling ($a = 0$), the only force on the walls comes from surface tension: the walls will straighten in order to minimize their radii within a given volume. When the average wall radius, $\bar{R}(t)$, is comparable to the linear dimensions of the confining volume (ℓ), the wall will stall or move exceedingly slowly. Given that left and right-handed life forms cannot coexist in the same domain, this simple model predicts, quite reasonably, that other factors in early-Earth's history have intervened to promote the observed homochirality.

Within the continuous description, the smallest volume is the correlation volume, $V_\xi \simeq 4\xi^3$, where the correlation length ξ is related to the potential $V(\mathcal{A})$ by $\xi^{-2} = V''(\mathcal{A} = \pm 1)$ [19]. The energy E_G required to flip a correlation-volume cell of a given chirality into one of opposite chirality is given by the energy barrier (ΔV) times the correlation volume: $E_G = V_\xi \Delta V$, where $\Delta V = |V(0) - V(\pm 1)|$. On the other hand, if E_f is the energy to flip the chirality of a single molecule and N_ξ is the average number of molecules in a correlation volume, then $E_G = N_\xi E_f$. Equating both expressions for E_G we obtain, $E_f = \frac{V_\xi}{N_\xi} \Delta V$.

From the expression for the potential, eq. 13, we obtain, with $f = 1$ and $g = 0$, $\Delta V = 0.193$ and $\xi = (k/\lambda_0)^{1/2}$, so that $V_\xi \simeq 4(k/\lambda_0)^{3/2}$. In order to estimate N_ξ , note that the parameters Q and k_S define the microscopic length-scale $\xi_{\text{micro}} = (Q/k_S)^{-1/6}$. Using $Q = 10^{15} \text{cm}^{-3} \text{s}^{-1}$ and $k_S = 10^{-25} \text{cm}^3 \text{s}^{-1}$, we obtain, $\xi_{\text{micro}} \simeq 2.154 \times 10^{-7} \text{cm}$ and $N_\xi \simeq (\xi/\xi_{\text{micro}})^3$. Thus, $E_f \simeq 4\xi_{\text{micro}}^3 \Delta V \simeq 7.7 \times 10^{-21} \text{cm}^3$.

This energy can be compared with the results from the numerical study of chiral symmetry breaking in GT, who found $a_c^2 \simeq 0.65(k/\lambda_0)^{3/2} \simeq 0.4 \text{cm}^3$. This is the critical energy for a correlation-volume cell to flip chirality. So, we must divide it by the number of molecules in a correlation volume in order to obtain the critical energy per molecule, $E_c^{\text{num}} \simeq 6.5 \times 10^{-21} \text{cm}^3$. The ratio of the two energies is, $E_f/E_c^{\text{num}} \simeq 1.18$, a nice agreement between the theoretical prediction from the Ginzburg criterion and the numerical results.

V. CHIRAL SELECTION AS A PHASE TRANSITION II: INCLUDING BIAS

Environmental effects, if above a certain threshold, may destroy any net chirality, restoring the system to a racemic state. Once external perturbations cease, the system will relax to its thermodynamically preferred state as it evolves toward final equilibrium. Within the present mean-field model, this evolution is characterized by a competition between left and right-handed domains separated by interfaces. This evolution is determined by the initial domain distribution and by the forces acting on the interfaces.

A. Percolation Constraints on Chiral Bias

One may think of the domains of each chirality as two competing populations immersed in an environment at "temperature" T . We use quotes to stress that this external influence may be attributed to several different sources of white noise with Gaussian amplitude a^2 . Consider a large volume $\mathcal{V} = V_L + V_R \gg V_\xi$, where $V_{L(R)}$ is the total volume in left(right) domains. If the fractional volumes of *both* left (V_L/\mathcal{V}) and right (V_R/\mathcal{V}) domains exceed a critical value p_c , they both percolate [32] and the total volume will be a convoluted structure similar to that of a sponge, with regions of left and right chirality separated by a thin interface. If, instead, only one of the two fractional volumes exceeds p_c , the volume will be percolated by the dominant handedness. The isolated domains of the opposite handedness will shrink and disappear.

Let $p_{L(R)}$ be the probability that a randomly chosen correlation-volume cell will be left(right)-handed. In thermal equilibrium, the relative probabilities obey, $p_L/p_R = \exp[-\Delta F/k_B T]$, where ΔF is the free-energy difference between the two populations. Of course, if they are equally probable (no bias), $p_L/p_R = 1$. Within the mean-field model, the free-energy difference between the two enantiometric phases is $\Delta F = \Lambda V_\xi$, $\Lambda \equiv |V(\mathcal{A}_L) - V(\mathcal{A}_R)|$, where $V(\mathcal{A}_{L(R)})$ is evaluated at the potential minima. For the potential of eq. 13 with $f = 1$, $\Lambda = 2g(1 - \pi/4)$.

For temperatures above the Ginzburg temperature (T_G), thermal fluctuations may drive the domains to flip their chiralities. As discussed in section 4.2, the associated energy scale is $E_G = k_B T_G \simeq V_\xi \Delta V$ [19]. Given that we will be mostly interested in very small biases ($\Delta V \gg \Lambda$), we may use the expression for ΔV obtained by taking $g = 0$. Thus, as the temperature drops below T_G , the chiral flipping is exponentially suppressed and the two populations are fixed by, $\frac{p_L}{p_R}|_{T < T_G} = \exp[-\frac{\Lambda}{\Delta V}]$. From the results above, with $f = 1$, we obtain $p_L/p_R|_{T_G} = \exp[-2g(1 - \pi/4)/0.193] \simeq \exp[-2.224g]$.

The ratio $p_L/p_R|_{T_G}$ sets the initial conditions for the subsequent dynamics of the system. The key point is whether one or both phases percolate. This is decided by comparing the probabilities $p_{L(R)}$ with the critical percolation probability, p_c . Now, p_c depends on dimensionality and somewhat less on the shape of the lattice cell. As an illustration, and to be consistent with the numerical simulations in GT which were performed on 3d cubic lattices, we take $p_c = 0.31$, the result for cubic lattices in 3d [32]. Using that $p_L + p_R = 1$, we obtain that for both phases

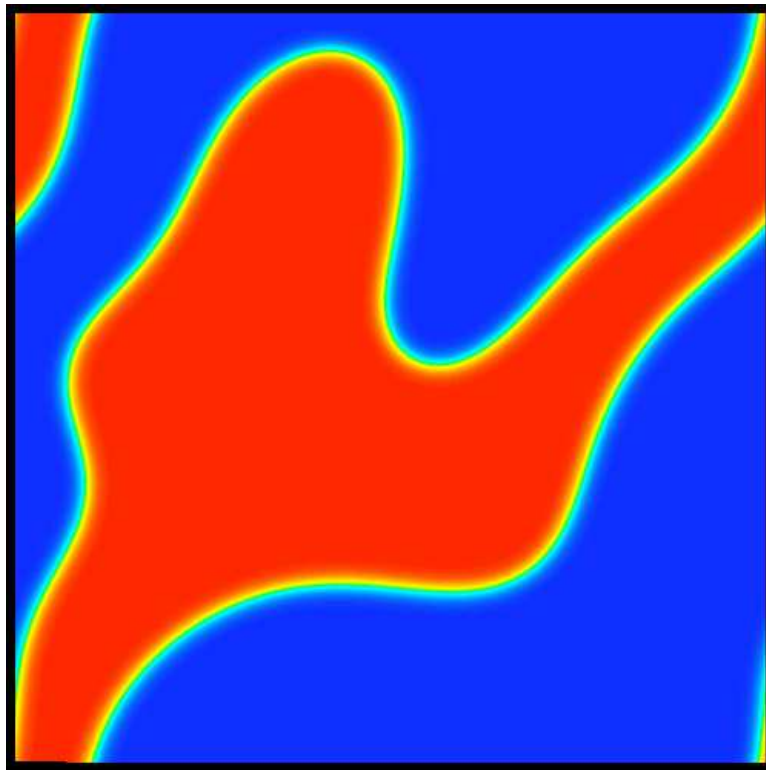


FIG. 3: Snapshot of evolution for $g = 0$, showing the two phases percolating the entire lattice and separated by a thin domain wall.

to percolate, $g \leq g_c = 0.36$. This is an upper bound on chiral bias in order for both types of domains to coexist and percolate throughout the volume. Clearly, if $g > 0.36$ only one domain percolates and chirality is firmly determined. However, unless some presently unknown effect strongly biases one enantiomer, g is most probably much smaller and both phases will initially percolate.

In figure 3 we show an example where both phases percolate, with $g = 0$. The reader can verify that each phase crosses the entire lattice, while the two phases are separated by a thin interface or domain wall. This 2d simulation used a 1024^2 lattice with periodic boundary conditions. For $g > 0.36$, only one of the two phases would percolate through the lattice: the minority phase would be constrained to form finite-volume domains that would shrink and disappear due to surface tension. We discuss wall dynamics next.

B. Wall Dynamics in the Presence of Bias

Once the flipping between phases ceases below T_G and percolation occurs, the wall network begins to evolve. Barring external influences, two forces will act on the walls: the curvature pressure p_s will act to straighten the walls, while the biasing pressure $p_g = \Lambda$ will tend to accelerate the walls toward the unfavored phase.

The curvature pressure can be written as $p_s \simeq \sigma/\bar{R}(t)$, where $\sigma = \sigma_0(k/\lambda_0)^{1/2}$ is the surface tension, with $\sigma_0 = \int dx_0 [\frac{1}{2}(\nabla_0 A_k)^2 + V(A_k)] = \int_{-1}^{+1} dA [2V(A)]^{1/2}$, and $\bar{R}(t)$ is its average radius. Using eq. 13 with $f = 1$ and $g = 0$, we obtain numerically that $\sigma_0 = 0.789$. [Corrections from a small g are quite negligible.]

At T_G , both the average wall curvature and separation will be of order of the correlation length $\xi = (k/\lambda_0)^{1/2}$. Thus, we can write

$$\frac{p_g}{p_s}|_{T_G} = \frac{2g(1 - \pi/4)}{\sigma_0} \simeq 0.544g. \quad (16)$$

Unless g is unrealistically large, the motion is initially dominated by the surface pressure and walls will tend to straighten before the biasing pressure becomes effective. There are thus two possibilities: given a large confining volume with linear length-scale ℓ , either p_g becomes active before the walls straighten to ℓ ($\bar{R} \rightarrow \ell$) or after. In

both cases, once p_g does become active, the walls will move toward the unfavored phase so that the volume $\sim \ell^3$ will eventually become homochiral.

The key question is thus whether this converting mechanism has enough time to take place in early-Earth given what we know of its prebiotic history and the magnitude of biasing sources proposed so far. In order to answer this question, we write the average wall radius as $\bar{R}(t) = \bar{R}_0(t)[k/\lambda_0]^{1/2}$ so that $p_g/p_s(t) = 0.544g\bar{R}_0(t)$, with $\bar{R}_0(t = t_G = 0) = 1$. In the last expression we set the time to zero at wall formation time. Thus, for the biasing pressure to dominate, the average wall radius must grow to satisfy $\bar{R}_c \geq [0.544g]^{-1}$: small values of g imply in very large radii. We must next estimate the time (t_g) it takes for this critical value to be achieved. The equation controlling the wall radius is

$$\frac{1}{\lambda_0} \frac{d\bar{R}}{dt} = \sigma \left(\frac{\xi}{\bar{R}(t)} \right). \quad (17)$$

The solution with $\bar{R}_0(0) = 1$ is

$$\bar{R}(t) = (k/\lambda_0)^{1/2} [1 + 2\sigma_0 t_0]^{1/2}. \quad (18)$$

Note that at formation time ($t_0 = 0$), the initial radius of the walls is equivalent to the correlation length and thus to the initial domain size as, $\bar{R}(0) = \xi = (k/\lambda_0)^{1/2}$. One can see how the initial length-scale in the problem depends on the two physical parameters, the diffusion coefficient k and the inverse time-scale λ_0 .

Substituting the critical value for the radius obtained above and solving for time,

$$t_{0g} = \frac{1}{2\sigma_0} \left[\left(\frac{p_s}{p_g} \Big|_{t_G} \right)^2 - 1 \right]. \quad (19)$$

Using the same values as before for Q , k_S and diffusivity in water, we obtain (taking $g \ll 1$), $t_g \simeq 4.8 \times 10^{-3} g^{-2} \text{y}$. [From here on, y is short for year, My(By) for millions(billions) of years, and Bya for billions of years ago.]

If we want life's early chirality to be decided, say, within 100 million years – sometime between the culmination of heavy bombardment period about 4Bya [13] and first life about 3.5 Bya [33], we obtain a lower bound on the biasing, $g \geq 7 \times 10^{-6} (100\text{My}/t_g)^{1/2}$. Values of g obtained from WNC are too small to promote homochirality on early Earth. The situation with CPL is not as clearcut, but it seems unlikely that such values of g can be sustained long enough due to the variability of possible astrophysical sources and the destruction of material by unpolarized UV light [2, 5] which might pass unfiltered through Earth's prebiotic atmosphere. A more detailed quantitative study is needed.

For $g \leq 10^{-6}$ it would take longer than the age of the Universe ($\simeq 14\text{By}$) before the biasing becomes active. Using t_g in the expression for $\bar{R}(t)$ above gives an estimate for the average radius of the interface by the time biasing pressure takes over the dynamics: $\bar{R}(t_g) \simeq (k/\lambda_0)^{1/2} (p_s/p_g)|_{t_G} \simeq 2g^{-1} \text{cm}$.

Once biasing pressure takes over, the interface will move toward the unfavored phase. We can estimate its velocity by studying the equation governing its motion [21]. Starting with the equation describing the spatiotemporal evolution of the chiral asymmetry, we look for a solution moving with constant velocity v , $\tilde{\mathcal{A}}(x - vt)$. The equation becomes,

$$\frac{k}{\lambda_0} \frac{\partial^2 \tilde{\mathcal{A}}}{\partial x^2} - \frac{\partial V}{\partial \tilde{\mathcal{A}}} = -\frac{v}{\lambda_0} \frac{\partial \tilde{\mathcal{A}}}{\partial x}, \quad (20)$$

where we assumed that the interface can be approximated by the propagation of a one dimensional front. This is justified considering that the thickness of the interface is of order ξ and thus *much* smaller than its average radius at $t > t_g$. Note also that upon switching space for time, the equation describes a particle moving in the presence of a velocity-dependent viscous force in a potential $-V(\mathcal{A})$. The solution satisfying the asymptotic boundary condition $\mathcal{A}(x \rightarrow \pm\infty) = \pm 1$ is determined by the interface's velocity v . Integrating eq. 20 by parts and using that the surface tension $\sigma = \int dx (\partial \mathcal{A} / \partial x)^2$ for $g \ll 1$, we obtain,

$$v = \frac{\Delta V}{\sigma_0} \lambda_0 \left(\frac{k}{\lambda_0} \right)^{1/2} \simeq 0.544g\lambda_0 \left(\frac{k}{\lambda_0} \right)^{1/2}, \quad (21)$$

where in the last identity we used the values for the potential of eq. 13. With the same fiducial values for k and λ_0 as before, $v \simeq 2.5g\text{my}^{-1}$. As an illustration, for the wall to convert a distance of 1km in 100My, $g \geq 4 \times 10^{-6}$. For the walls to sweep a distance equivalent to Earth's radius, $g \geq 2.6 \times 10^{-2}$. A small bias doubly compromises the conversion of racemic prebiotic chemistry to homochirality: i) the time for the bias to take over, $t_g \simeq 4.8 \times 10^{-3} g^{-2} \text{y}$ can easily exceed the age of the Universe even for values of the bias much larger than the ones proposed thus far; and ii) once the bias takes over, the distance swept by the wall, $d_{\text{wall}}(t) \simeq 2.5g(t/y)\text{m}$, can be exceedingly small even for large times of order 100My.

C. Nucleation-Induced Homochirality in Prebiotic Environments

Given that for small bias the wall motion will not set in for a very long time, it is legitimate to ask whether the conversion to the final homochiral phase may happen via homogeneous nucleation [14, 20]. In this case, a nucleus of the favored phase will thermally nucleate within the unfavored phase with a rate per unit volume $\Gamma(T, g)$ controlled by the Arrhenius factor

$$\Gamma \simeq \lambda_0 (\lambda_0/k)^{3/2} \exp[-E_g(\mathcal{A}_b)/k_B T], \quad (22)$$

where $E_g(\mathcal{A}_b)$ is the energy of the so-called ‘‘bounce’’ or critical nucleus. In the thin-wall approximation, valid in the limit of small asymmetry between the two cases and thus here ($\Lambda/\Delta V \ll 1$), the energy of the bounce of radius R is well-approximated by $E(R) = -\frac{4\pi}{3}R^3\Delta V + 4\pi R^2\sigma$. Extremizing this expression, we find, for the radius of the critical nucleus and its associated energy, $R_c = 2\sigma/\Delta V \simeq 1.84g^{-1}(k/\lambda_0)^{1/2}$ and $E(R_c) = \frac{16\pi}{3}\frac{\sigma^3}{(\Delta V)^2} \simeq 44.5g^{-2}(k/\lambda_0)^{3/2}$, where in the last expressions we used the potential of eq. 13. Note how $E(R_c) \propto g^{-2}$. From the expression for the nucleation rate we can estimate the time-scale for nucleation in a given prebiotic volume V_{pb} as

$$\tau_{\text{nuc}} \simeq (\Gamma V_{pb})^{-1} \simeq 1.3 \times 10^{-15} \left(\frac{10^6 \text{m}^3}{V_{pb}} \right) \exp[89/g^2 a^2] \text{y}, \quad (23)$$

where the last expression was obtained using the usual fiducial values for k and λ_0 and the relation $a^2 = 2k_B T$ for the environmental fluctuation-inducing noise amplitude.

Given that the nucleation time-scale decreases with volume, as an illustration let us consider a large volume of the unbiased phase, say a ‘‘shallow’’ cylindrical pool with volume $V_{pb} = \pi(10^3 \text{m})^2(100 \text{m}) = \pi \times 10^8 \text{m}^3$. Within this volume, $\tau_{\text{nuc}} \simeq 4 \times 10^{-18} \exp[89/g^2 a^2] \text{y}$. If we impose, realistically, that $\tau_{\text{nuc}} \leq 100 \text{My}$, we obtain a bound on the critical nucleation barrier $E(R_c)/k_B T \leq 58.5$. For small asymmetries, this bound cannot be satisfied. Indeed, in terms of the asymmetry g , and using that a typical noise amplitude capable of inducing sizeable fluctuations is $a^2 \simeq 0.5$ (cf. GT), we obtain $g \geq 1.74$, an unrealistically large value. For a volume with extension comparable to the Earth’s radius, $V_{pb} = \pi(6.5 \times 10^6 \text{m})^2(100 \text{m}) = 1.3 \times 10^{16} \text{m}^3$, the bound becomes $g \geq 1.53$. We conclude that homogeneous nucleation cannot resolve the chirality issue. It remains to be seen if environmental disturbances may promote a faster nucleation rate [11].

VI. SUMMARY AND OUTLOOK

The spatiotemporal evolution of prebiotic homochirality was investigated in the context of an autocatalytic reaction network featuring enantiometric cross-inhibition catalysed by dimers and chiral bias. Domains of opposite chirality, separated by thin interfaces, compete for dominance. It was shown that the dynamics of the domain network is determined by the percolation properties of its initial distribution and subsequently by the two main forces acting on the interfaces, surface tension and chiral bias. Small biases of $g \leq 10^{-6}$ were shown to be inefficient to drive reasonably-sized reactor pools toward homochirality within presently-accepted time-scales for the origin of life on Earth. As a consequence, the present calculations indicate that WNCs cannot explain the observed homochirality of life’s biomolecules. CPL remains a remote possibility, albeit current sources do not look promising either in magnitude and duration. Also, it should be noted that unpolarized UV may destroy any early enantiometric excess.

The results obtained assume that the polymerization dynamics can be captured by truncating the reaction network to $n \leq 2$ and that the dynamics of dimers is enslaved by that of monomers (the adiabatic approximation). These approximations imply that complete chiral separation can only occur with perfect fidelity $f = 1$. Going beyond involves solving the complete network of spatiotemporal rate equations for larger values of n and for varying fidelity, a computer-intensive, but not impossible, task. However, given that the formation rate of higher n polymers will necessarily be slower, we believe that the results obtained here capture at least qualitatively the essentials of the more general case. It remains a challenging open question whether a simple transformation could be found to reduce the biased higher- n system to an effective field theory as done here for $n = 2$.

What other possible sources of bias could have driven Earth’s prebiotic chemistry toward homochirality? We cannot rule out the possibility that some unknown chemical bias satisfying the above bound might have been active. Another, highly unattractive, possibility is that an unlikely large statistical fluctuation towards one enantiometer did occur and established the correct initial conditions. Possible bombardment from meteors contaminated with chiral compounds could also have jump-started the process, although one still needs to explain how the chiral excess formed in the meteors in the first place.

It seems to us that the answer to this enigma will be found in the coupling of the reaction network to the environment. We note again that the results obtained here are within the diffusive, and hence ‘‘gentle,’’ evolution towards

homochirality. Early-Earth, however, was a dramatic environment. Given the nonlinear properties of the spatiotemporal equations describing the evolution towards homochirality, environmental disturbances, such as meteoritic impacts or volcanic eruptions, must have played a key role in early-Earth's prebiotic chemistry. These disturbances, if violent enough, would certainly affect the evolution of the chiral domain network and possibly change the bounds obtained in the present work. Gleiser and Thorarinson proposed to model the coupling to an external disturbance stochastically [12]. Within their framework, results will depend on how the amplitude of the external "noise" compares with the critical value described in section 4.1. Preliminary results indicate that large enough noises (modelling external influences) may redirect the direction of homochirality entirely, erasing any previous evolution toward either handedness. Further work along these lines is underway. In a different approach, Brandenburg and Multamäki suggested that hydrodynamic turbulence could have sped up the march toward homochirality [6]. In either case, it is clear that the evolution toward homochirality, as that of life itself, cannot be separated from Earth's early environmental history.

The author thanks Gustav Arrhenius, Jeffrey Bada, Freeman Dyson, Leslie Orgel, and Joel Thorarinson for stimulating discussions. He also thanks Joel Thorarinson for producing figure 3.

-
- [1] Avetisov, V. A. and Goldanskii, V.:1993, Chirality and the Equation of Biological Big Bang. *Phys. Lett.*, **A 172**, 407–410.
- [2] Bailey, J.:2001, Astronomical sources of circularly polarized light and the origin of homochirality. *Orig. Life Evol. Biosph.* **31**, 167–183.
- [3] Bakasov, A., Ha, T.-K., and Quack, M.:1998, Ab initio calculation of molecular energies including parity violating interactions. *J. Chem. Phys.* **109**, 7263–7285.
- [4] Blackmond, D. G.:2004, Asymmetric autocatalysis and its implications for the origin of homochirality. *PNAS* **101**, 5732–5736.
- [5] Bonner, W. A.:1996, The Quest for Chirality. In David . D. Cline, editor, *Physical Origin of Homochirality in Life*, Santa Monica, California, February 1995. AIP Conference Proceedings 379, AIP Press, New York.
- [6] Brandenburg, A. & Multamäki, T.:2004, How Long Can Left and Right Handed Life Forms Coexist?. *Int. J. Astrobiol.*, **3**, 209–219.
- [7] Dunitz, J. D.:1996, Symmetry Arguments in Chemistry. *PNAS* **93**, 14260–14266.
- [8] Engel, M. H. and Macko, S. A.:1997, Isotopic evidence for extraterrestrial non-racemic amino acids in the Murchison meteorite. *Nature* **389**, 265–268.
- [9] Frank, F. C.:1953, On Spontaneous Asymmetric Catalysis. *Biochim. Biophys. Acta*, **11**, 459–463.
- [10] Gayathri, V. S.. and Rao, M.:2005, Fluctuation Induced Chiral Symmetry Breaking in Autocatalytic Reaction-Diffusion Systems. *arXiv:cond-mat/0503176*
- [11] Gleiser, M. and Howell, R.:2005, Resonant Nucleation. *Phys. Rev. Lett.* **94**, 151601.
- [12] Gleiser, M. and Thorarinson, J.:2006, Prebiotic homochirality as a critical phenomenon. in press *Orig. Life Evol. Biosph.* *arXiv: astro-ph/0601399*.
- [13] Gomes, R. *et al.*:2005, Origin of the cataclysmic late heavy bombardment period of the terrestrial planets. *Nature* **435**, 466–469.
- [14] Gunton, J. D., San Miguel, M., and Sahni, P. S.:1983, In C. Domb and J. L. Lebowitz, editors *Phase Transitions and Critical Phenomena v. 8*, Academic Press, London.
- [15] Haken, H.:1983, *Synergetics: An Introduction*. Springer-Verlag, Berlin.
- [16] Kondepudi, D. K. and Nelson, G. W.:1983, Chiral Symmetry Breaking in Nonequilibrium Systems. *Phys. Rev. Lett.*, **50**, 1023–1026.
- [17] Kondepudi, D. K. and Nelson, G. W.:1985, Weak Neutral Currents and the Origin of Biomolecular Chirality. *Nature*, **314**, 438–441.
- [18] Kondepudi, D. K.:1996, *Physical Origin of Homochirality in Life*. In David . D. Cline, editor, *Physical Origin of Homochirality in Life*, Santa Monica, California, February 1995. AIP Conference Proceedings 379, AIP Press, New York.
- [19] Landau, L. D. and Lifshitz, E. M.:1980, *Statistical Physics 3rd Edition, Part I*. Pergamon Press, New York.
- [20] Langer, J. S.:1967, Theory of the Critical Point. *Ann. Phys. (NY)* **41**, 108–157.
- [21] Langer, J. S.:1992, An introduction to the kinetics of first-order phase transitions. In C. Godrèche, editor, *Solids Far from Equilibrium*, (Cambridge University Press, Cambridge).
- [22] Lazzeretti, P., Zanasi R., and Faglioni F.:1999, Energetic stabilization of d-camphor via weak neutral currents. *Phys. Rev. E* **60**, 871–874.
- [23] Lucas, P. W. *et al.*:2005, UV Circular Polarization in Star Formation Regions: The Origin of Homochirality?. *Orig. Life Evol. Biosph.*, **35**, 29–60.
- [24] Nilsson, M., Brandenburg, A., Andersen, C., and Höfner, S.:2005, Uni-directional polymerization leading to homochirality in the RNA world. *Orig. Life Evol. Biosph.* **35**, 225–241.
- [25] Orgel, L. E.:1998, The Origin of Life – How Long Did It Take?. *Orig. Life Evol. Biosph.*, **28**, 91–96.
- [26] Pizzarello, S. and Cronin, J. R.:1998, Alanine enantiomers in the Murchison meteorite. *Nature* **394**, 236.
- [27] Plasson, R., Bersini, H., and Commeyras, A.:2004, Recycling Frank: Spontaneous emergence of homochirality in noncatalytic systems. *PNAS* **101**, 16733–16738.

- [28] Saito, Y. and Hyuga, H.:2004, Homochirality Proliferation in Space. *J. Phys. Soc. Jap.*, **73**, 1685–1688.
- [29] Salam, A.:1991, The Role of Chirality in the Origin of life. *J. Mol. Evol.*, **33**, 105–113.
- [30] Sandars, P. G. H.:2003, A Toy Model for the Generation of Homochirality During Polymerization. *Orig. Life Evol. Biosph.*, **33**, 575–587.
- [31] Soai, K., Shibata, T., Morioka, H. and Choji, K.:1995, Asymmetric autocatalysis and amplification of enantiometric excess of a chiral molecule. *Nature* **378**, 767–768.
- [32] Stauffer, D.:1979, Percolation Theory. *Phys. Rep.* **54**, 1–74.
- [33] van Zuilen, M. A., Lepland, A., and Arrhenius, G.:2002, Reassessing the evidence for the earliest traces of life. *Nature* **420**, 202.
- [34] Wattis, J. A. and Coveney, P. V.:2005, Symmetry-Breaking in Chiral Polymerization. *Orig. Life Evol. Biosph.*, **35**, 243–273.
- [35] Yamagata, Y.:1966, A hypothesis for the asymmetric appearance of biomolecules on earth *J. Theoret. Biol.* **11**, 495–498.